Prior-Based Multi Material Decomposition for Dual Energy CT

Sabrina Dorn[1,2], Shuqing Chen[3], Stefan Sawall[1,2], Joscha Maier[1,2], Michael Knaup[1], Andreas Maier[3], Michael Lell[4], and Marc Kachelrieß[1,2]

[1]German Cancer Research Center (DKFZ), Heidelberg, Germany
[2]University of Heidelberg, Germany
[3]Friedrich-Alexander University Erlangen-Nürnberg, Germany
[4]Hospital Nürnberg, Paracelsus Medical University

DEUTSCHES KREBSFORSCHUNGSZENTRUM IN DER HELMHOLTZ-GEMEINSCHAFT

Aim

To propose a prior-based multi material decomposition consisting of multiple organ-dependent three material decompositions for DECT data

Common Image-Domain Material Decompositions

$$\boldsymbol{f}(\boldsymbol{r}) = (f_{\mathrm{H}}(\boldsymbol{r}), f_{\mathrm{L}}(\boldsymbol{r}))$$

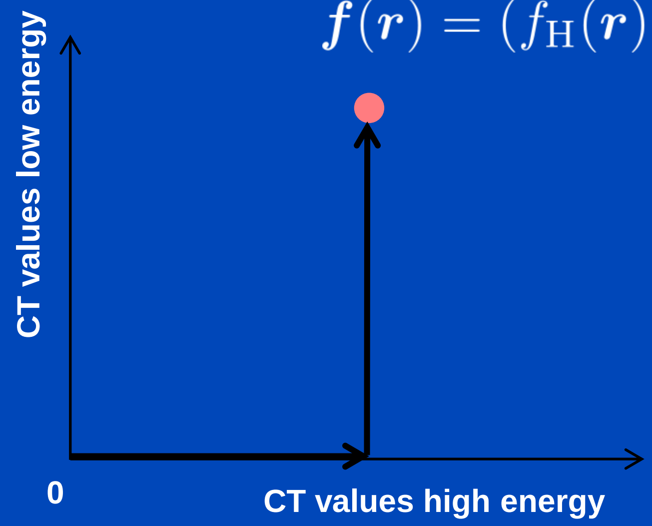

Common Image-Domain Material Decompositions

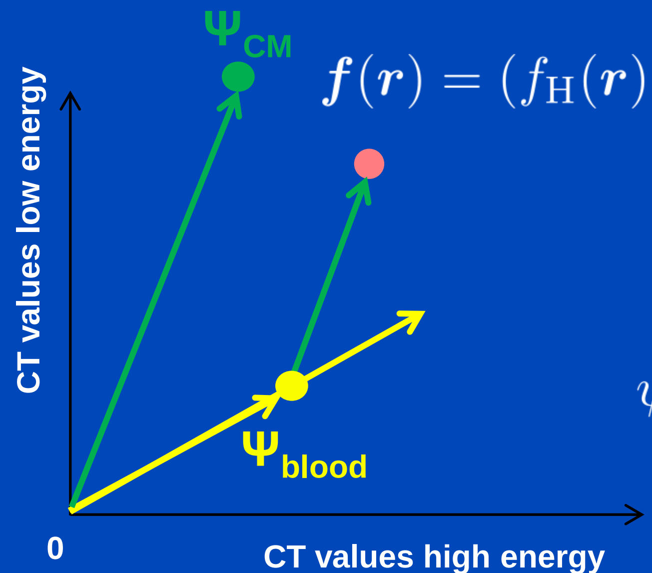

$$\boldsymbol{f}(\boldsymbol{r}) = (f_{\mathrm{H}}(\boldsymbol{r}), f_{\mathrm{L}}(\boldsymbol{r}))$$

Basis material vectors:

$$\psi_{\mathrm{CM}} = (\psi_{\mathrm{H,CM}}, \psi_{\mathrm{L,CM}})$$

$$\psi_{\mathrm{blood}} = (\psi_{\mathrm{H,blood}}, \psi_{\mathrm{L,blood}})$$

CM: contrast media

Two material decomposition (2MD)

$$\begin{pmatrix} f_{\mathrm{L}}(\boldsymbol{r}) \\ f_{\mathrm{H}}(\boldsymbol{r}) \end{pmatrix} = \begin{pmatrix} \psi_{\mathrm{L,\ blood}} & \psi_{\mathrm{L,\ CM}} \\ \psi_{\mathrm{H,\ blood}} & \psi_{\mathrm{H,\ CM}} \end{pmatrix} \cdot \begin{pmatrix} f_{\mathrm{blood}}(\boldsymbol{r}) \\ f_{\mathrm{CM}}(\boldsymbol{r}) \end{pmatrix}$$

Common Image-Domain Material Decompositions

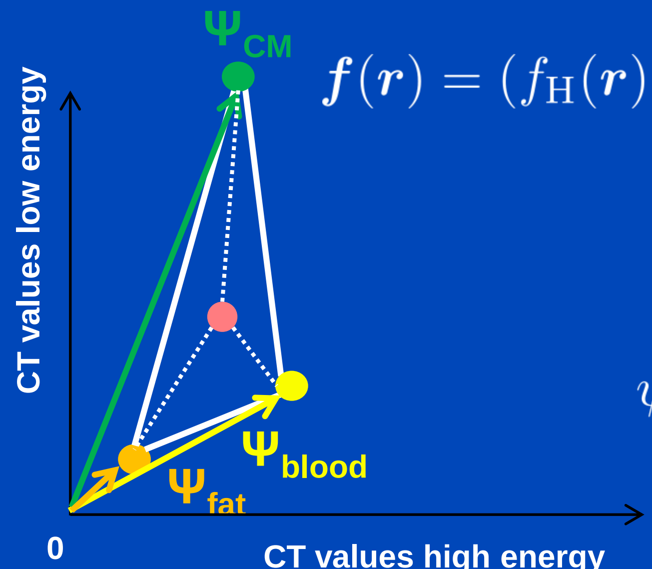

$$\boldsymbol{f}(\boldsymbol{r}) = (f_\mathrm{H}(\boldsymbol{r}), f_\mathrm{L}(\boldsymbol{r}))$$

Basis material vectors:

$$\psi_\mathrm{CM} = (\psi_\mathrm{H,CM}, \psi_\mathrm{L,CM})$$
$$\psi_\mathrm{blood} = (\psi_\mathrm{H,blood}, \psi_\mathrm{L,blood})$$
$$\psi_\mathrm{fat} = (\psi_\mathrm{H,fat}, \psi_\mathrm{L,fat})$$

CM: contrast media

Three material decomposition (3MD)

$$\begin{pmatrix} f_\mathrm{L}(\boldsymbol{r}) \\ f_\mathrm{H}(\boldsymbol{r}) \\ 1 \end{pmatrix} = \begin{pmatrix} \psi_\mathrm{L,\ CM} & \psi_\mathrm{L,\ blood} & \psi_\mathrm{L,\ fat} \\ \psi_\mathrm{H,\ CM} & \psi_\mathrm{H,\ blood} & \psi_\mathrm{H,\ fat} \\ 1 & 1 & 1 \end{pmatrix} \cdot \begin{pmatrix} f_\mathrm{CM}(\boldsymbol{r}) \\ f_\mathrm{blood}(\boldsymbol{r}) \\ f_\mathrm{fat}(\boldsymbol{r}) \end{pmatrix}$$

Volume conservation constraint

Prior Work

- **Multi material decomposition (MMD)**
  - **Tessellation of multiple triangles**
  - **“A library of material triplets”**
  - **Each voxel is assigned to one triangle**

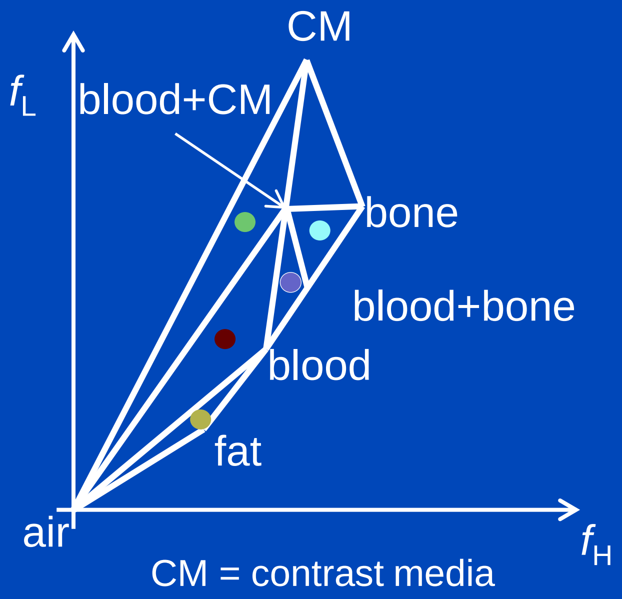

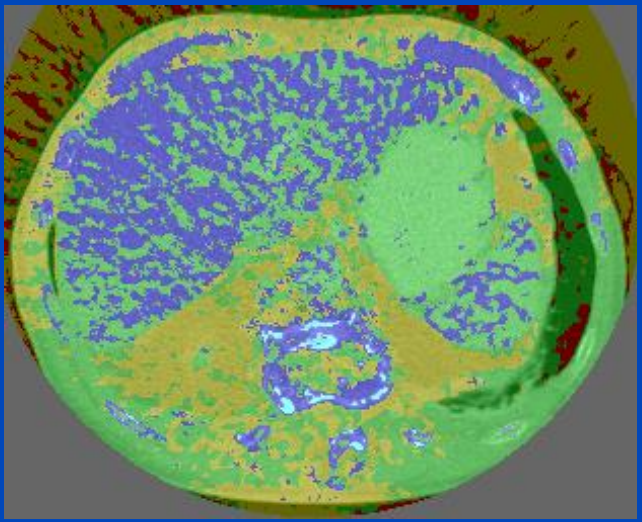

  - **Some voxels are misrepresented by the basis materials**
  - **Every voxel is evaluated independently**
  - **No local information is taken into account**

Mendonça et al.
A Flexible Method for Multi-Material Decomposition of Dual-Energy CT Images. IEEE TMI 33(1):99-116, 2014.

Prior Work

- **Segmentation-assisted material quantification (SAMQ):**
  - **Thresholding of the data set into different tissue classes**
  - **Locally adapted material decomposition**
  - **Many basis materials: air, fat, liver/blood, CM, CaHA, …**

CT Image

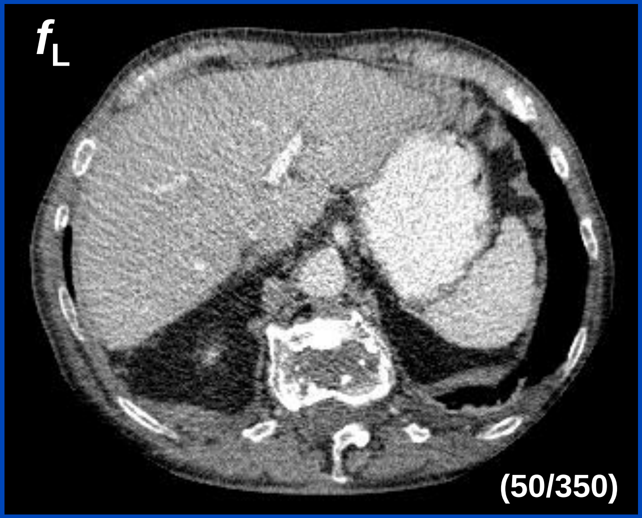

Segmentation

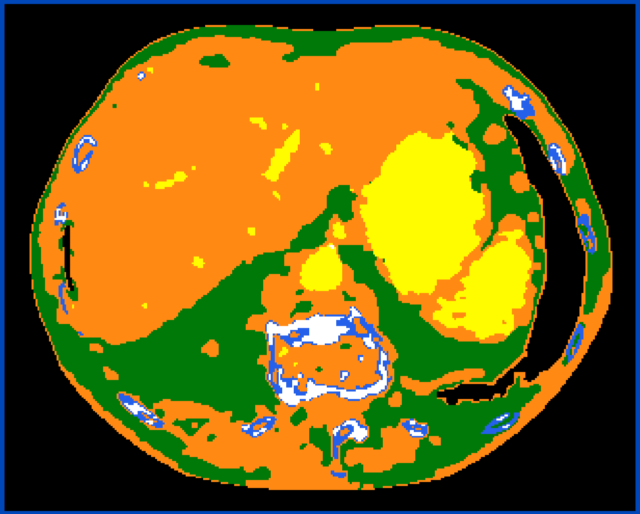

- **Naïve segmentation approach → ambiguities in the decomposition**

Prior Work

- **Context-sensitive CT Imaging**

Multi-organ segmentation

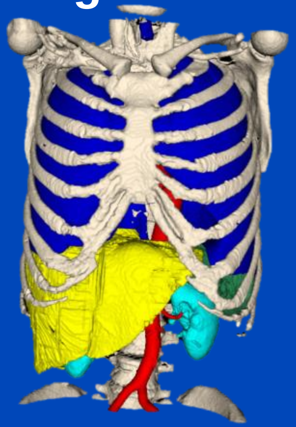

Binary mask for each anatomical structure, e. g.:

heart	lung	muscle	bone	fat

→ Masks to allow for individual settings for each organ

- **Organ-specific reconstruction**

- **High spatial resolution in lung and bone**
- **Low noise level in soft tissue**

Dorn and Kachelrieß et al.
Organ-Specific Context-Sensitive CT Image Reconstruction and Display. SPIE 2018.

Prior Work

- Context-sensitive CT Imaging

Multi-organ segmentation

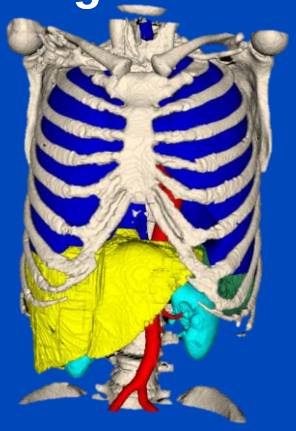

Binary mask for each anatomical structure, e. g.:

→ **Masks to allow for individual settings for each organ**
- **Organ-specific reconstruction**
- **Organ-specific display**

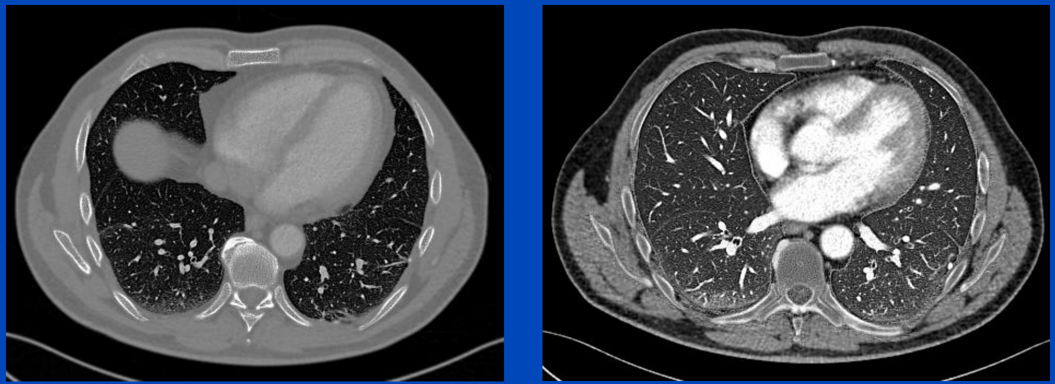

Adaptive windowing

Different window level settings for each organ

- **Bone window in bone**
- **Lung window in lung**
- **Body window in soft tissue**

Prior Work

- **Context-sensitive CT Imaging**

Multi-organ segmentation

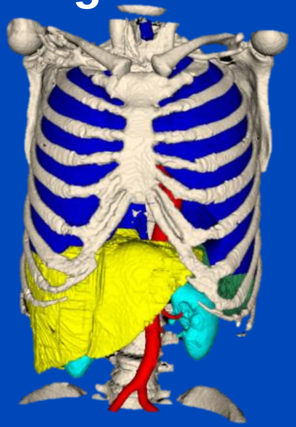

Binary mask for each anatomical structure, e. g.:

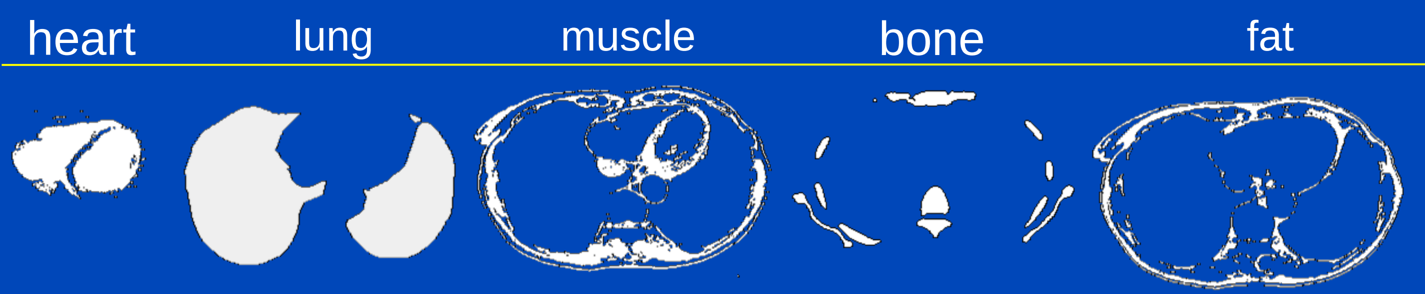

→ Masks to allow for individual settings for each organ

- **Organ-specific reconstruction**
- **Organ-specific display**

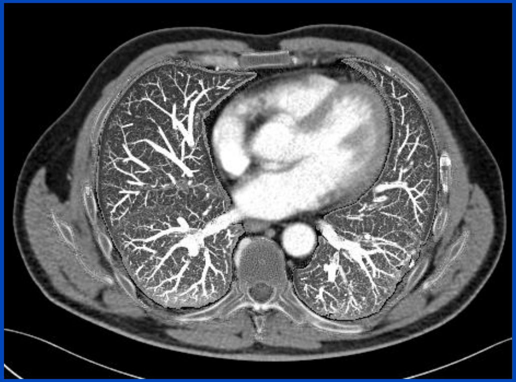

Adaptive sliding thin slab

Mean intensity projection in soft tissue (5 mm)

Maximum intensity projection in lung (10 mm)

Prior Work

- **Context-sensitive CT Imaging**

Multi-organ segmentation

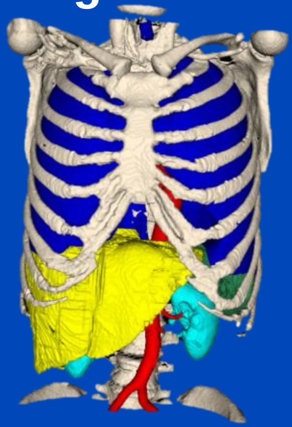

Binary mask for each anatomical structure, e. g.:

heart	lung	muscle	bone	fat

→ Masks to allow for individual settings for each organ

- **Organ-specific reconstruction**
- **Organ-specific display**
- **Organ-specific DE evaluation**

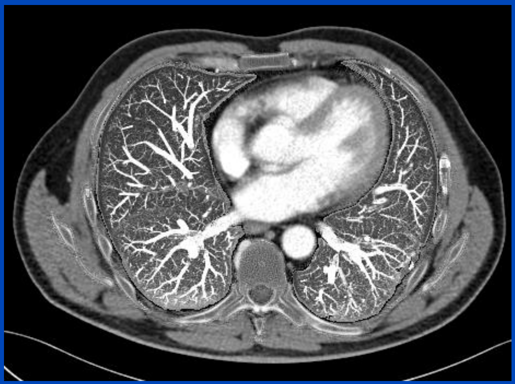

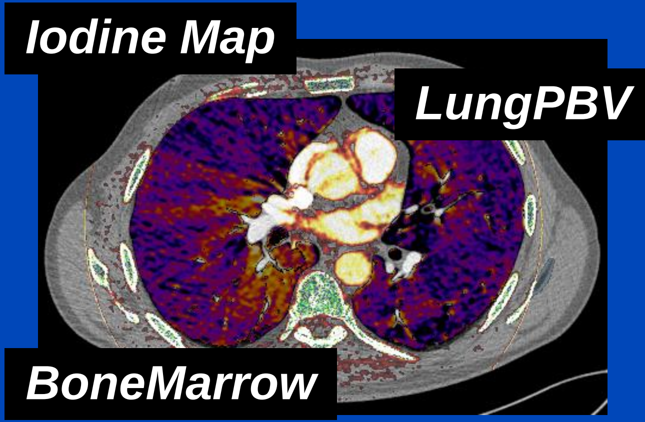

Dorn and Kachelrieß et al.
Organ-Specific Context-Sensitive CT Image Reconstruction and Display. SPIE 2018.

Prior Anatomical Knowledge

- **Automatic multi-organ segmentation**
- **Cascaded 3D fully convolutional neural network consisting of two successive stages**

Poster Session, Wednesday 2:00 p.m. – 4:20 p.m.

- **Automatic segmentation of liver, kidneys and spleen**
- **Thresholding of remaining voxels into following structures: lung, muscles, fat, bone and vasculature**

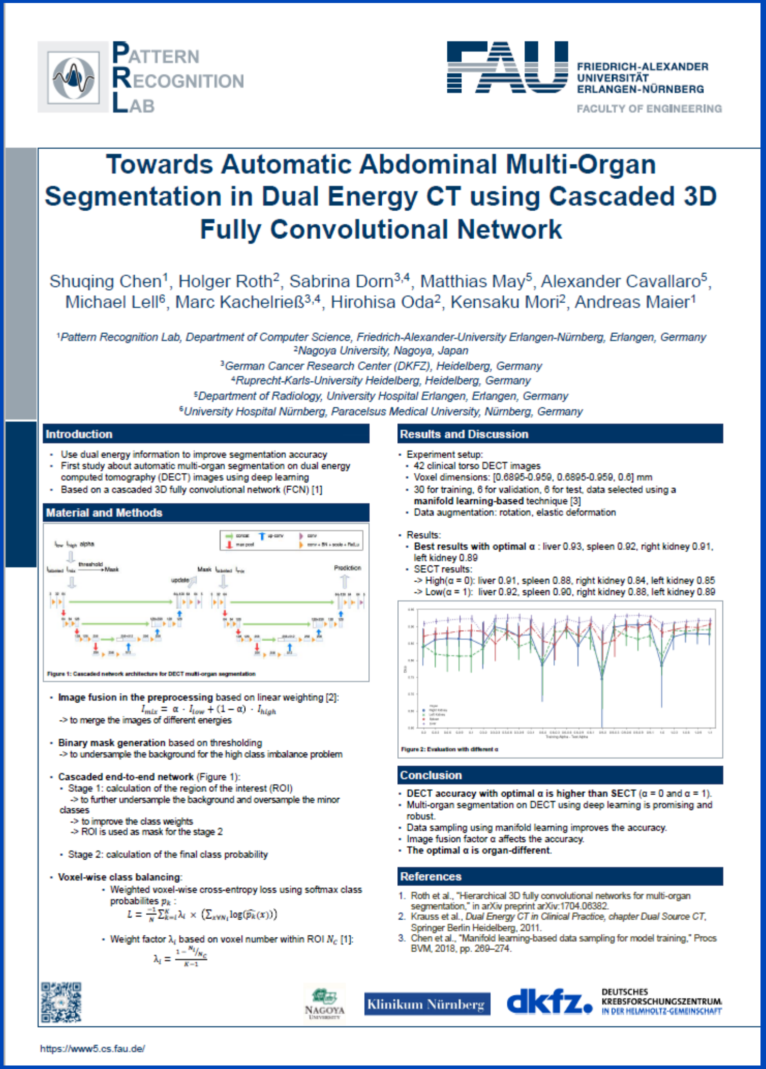

PATTERN RECOGNITION LAB

FAU FRIEDRICH-ALEXANDER UNIVERSITÄT ERLANGEN-NÜRNBERG

FACULTY OF ENGINEERING

Towards Automatic Abdominal Multi-Organ Segmentation in Dual Energy CT using Cascaded 3D Fully Convolutional Network

Shuqing Chen[1], Holger Roth[2], Sabrina Dorn[3,4], Matthias May[5], Alexander Cavallaro[5], Michael Lell[6], Marc Kachelrieß[3,4], Hirohisa Oda[2], Kensaku Mori[2], Andreas Maier[1]

[1]*Pattern Recognition Lab, Department of Computer Science, Friedrich-Alexander-University Erlangen-Nürnberg, Erlangen, Germany*
[2]*Nagoya University, Nagoya, Japan*
[3]*German Cancer Research Center (DKFZ), Heidelberg, Germany*
[4]*Ruprecht-Karls-University Heidelberg, Heidelberg, Germany*
[5]*Department of Radiology, University Hospital Erlangen, Erlangen, Germany*
[6]*University Hospital Nürnberg, Paracelsus Medical University, Nürnberg, Germany*

Introduction

- Use dual energy information to improve segmentation accuracy
- First study about automatic multi-organ segmentation on dual energy computed tomography (DECT) images using deep learning
- Based on a cascaded 3D fully convolutional network (FCN) [1]

Material and Methods

Figure 1: Cascaded network architecture for DECT multi-organ segmentation

- **Image fusion in the preprocessing** based on linear weighting [2]:
  $$I_{mix} = \alpha \cdot I_{low} + (1-\alpha) \cdot I_{high}$$
  -> to merge the images of different energies
- **Binary mask generation** based on thresholding
  -> to undersample the background for the high class imbalance problem
- **Cascaded end-to-end network** (Figure 1):
  - Stage 1: calculation of the region of the interest (ROI)
    -> to further undersample the background and oversample the minor classes
    -> to improve the class weights
    -> ROI is used as mask for the stage 2
  - Stage 2: calculation of the final class probability
- **Voxel-wise class balancing**:
  - Weighted voxel-wise cross-entropy loss using softmax class probabilites p_k :
    $$L = \frac{-1}{N}\sum_{k=1}^{K}\lambda_i \times \left(\sum_{x \forall N_i}\log(\widehat{p_k}(x))\right)$$
  - Weight factor λ_i based on voxel number within ROI N_C [1]:
    $$\lambda_i = \frac{1-{N_i}/{N_C}}{K-1}$$

Results and Discussion

- Experiment setup:
  - 42 clinical torso DECT images
  - Voxel dimensions: [0.6895-0.959, 0.6895-0.959, 0.6] mm
  - 30 for training, 6 for validation, 6 for test, data selected using a **manifold learning-based** technique [3]
  - Data augmentation: rotation, elastic deformation
- Results:
  - **Best results with optimal α** : liver 0.93, spleen 0.92, right kidney 0.91, left kidney 0.89
  - SECT results:
    -> High(α = 0): liver 0.91, spleen 0.88, right kidney 0.84, left kidney 0.85
    -> Low(α = 1): liver 0.92, spleen 0.90, right kidney 0.88, left kidney 0.89

Figure 2: Evaluation with different α

Conclusion

- **DECT accuracy with optimal α is higher than SECT** (α = 0 and α = 1).
- Multi-organ segmentation on DECT using deep learning is promising and robust.
- Data sampling using manifold learning improves the accuracy.
- Image fusion factor α affects the accuracy.
- **The optimal α is organ-different.**

References

1. Roth et al., "Hierarchical 3D fully convolutional networks for multi-organ segmentation," in arXiv preprint arXiv:1704.06382.
2. Krauss et al., *Dual Energy CT in Clinical Practice, chapter Dual Source CT*, Springer Berlin Heidelberg, 2011.
3. Chen et al., "Manifold learning-based data sampling for model training," Procs BVM, 2018, pp. 269–274.

NAGOYA UNIVERSITY
Klinikum Nürnberg
dkfz. DEUTSCHES KREBSFORSCHUNGSZENTRUM IN DER HELMHOLTZ-GEMEINSCHAFT

https://www5.cs.fau.de/

Prior-Based Multi Material Decomposition (PBMMD)

- **Multi material decomposition**
  - **Adjust the basis materials to the organ of interest exploiting the prior information**
  - **Perform for each organ a three material decomposition (3MD)**

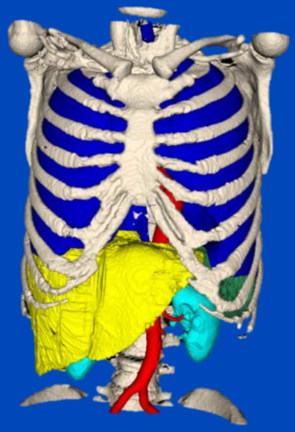

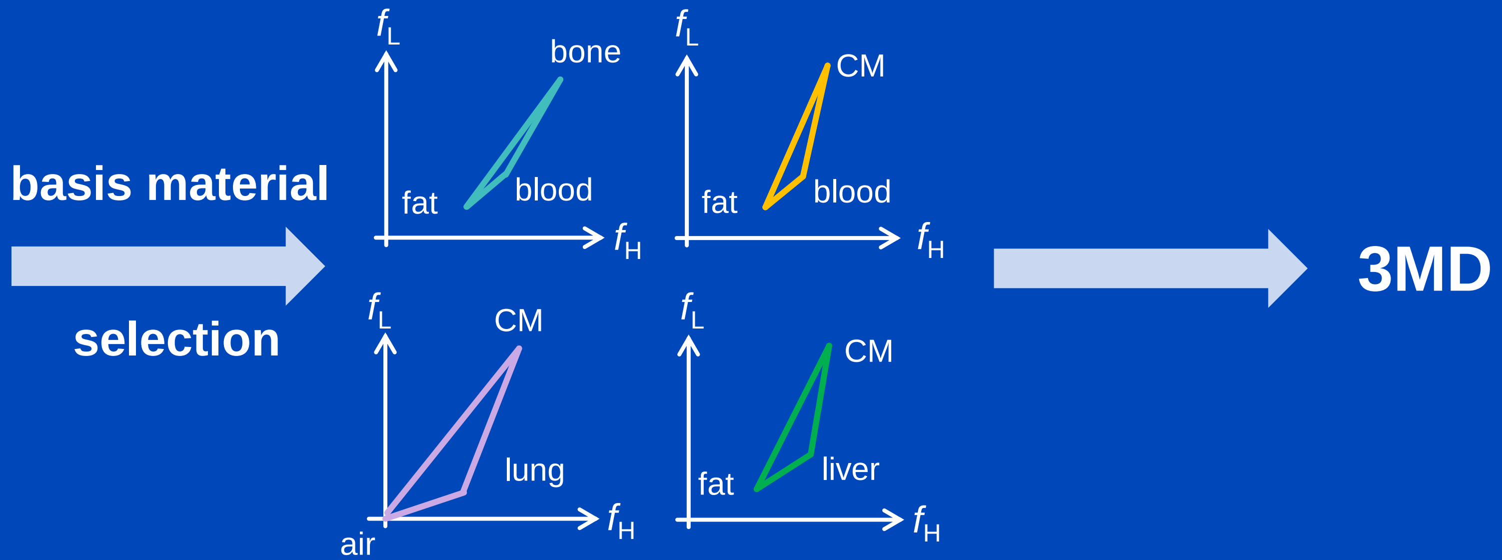

Prior-Based Multi Material Decomposition (PBMMD)

- Assuming each voxel is a compound of three basis materials that are known a-priori.
- Assuming the mixture is volume preserving, meaning that all volume fractions sum up to one (volume conservation constraint):

$$\begin{pmatrix} f_{\mathrm{L}}(\boldsymbol{r}) \\ f_{\mathrm{H}}(\boldsymbol{r}) \\ 1 \end{pmatrix} = \begin{pmatrix} \psi_{\mathrm{L},\,1} & \psi_{\mathrm{L},\,2} & \psi_{\mathrm{L},\,3} \\ \psi_{\mathrm{H},\,1} & \psi_{\mathrm{H},\,2} & \psi_{\mathrm{H},\,3} \\ 1 & 1 & 1 \end{pmatrix} \cdot \begin{pmatrix} f_1(\boldsymbol{r}) \\ f_2(\boldsymbol{r}) \\ f_3(\boldsymbol{r}) \end{pmatrix}$$

- Each volume fraction has to satisfy the condition (positivity constraint)

$$f_i(\boldsymbol{r}) \geq 0$$

- Direct inversion of the LSE with noise compensating projections

O'Donnell et al. Material decomposition in an arbitrary number of dimensions using noise compensating projection. Biomed. Phys. Eng Express 2018

Prior-Based Multi Material Decomposition (PBMMD)

- **Basis materials are adapted to the organ of interest**
- **Overlapping triangles in the DE space**

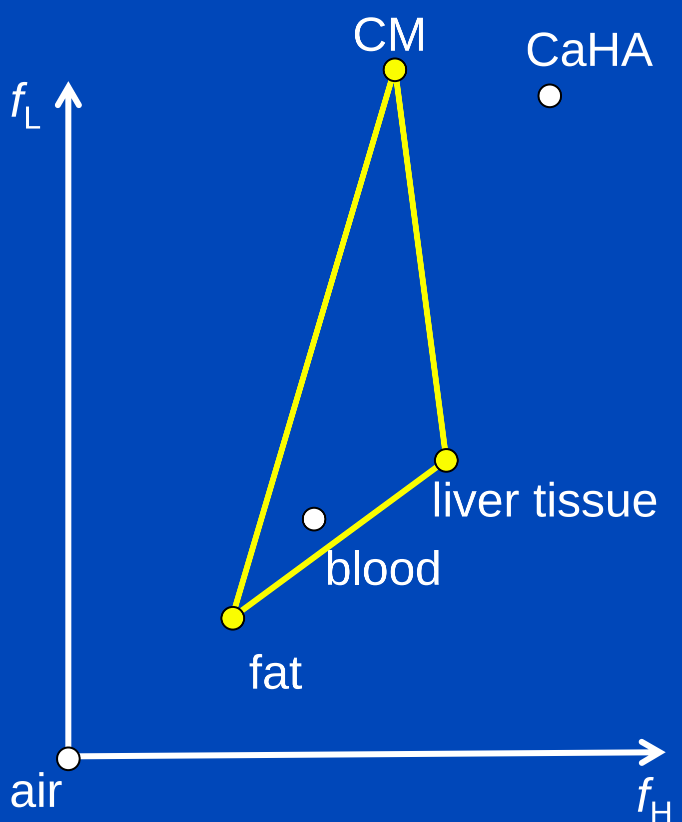

liver:

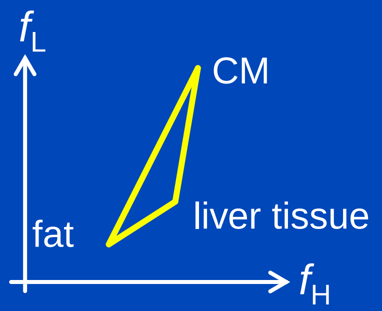

Prior-Based Multi Material Decomposition (PBMMD)

- **Basis materials are adapted to the organ of interest**
- **Overlapping triangles in the DE space**

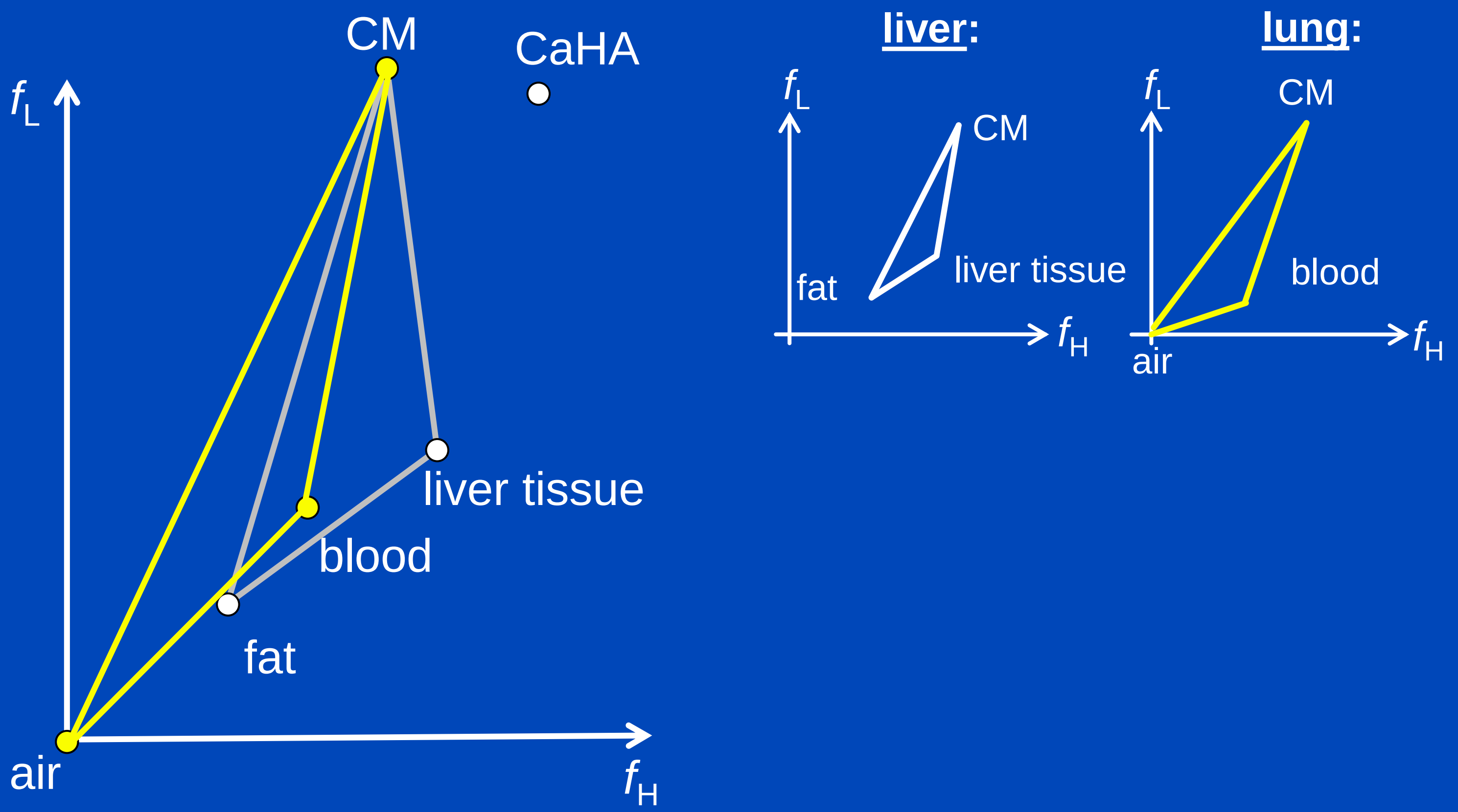

Prior-Based Multi Material Decomposition (PBMMD)

- **Basis materials are adapted to the organ of interest**
- **Overlapping triangles in the DE space**

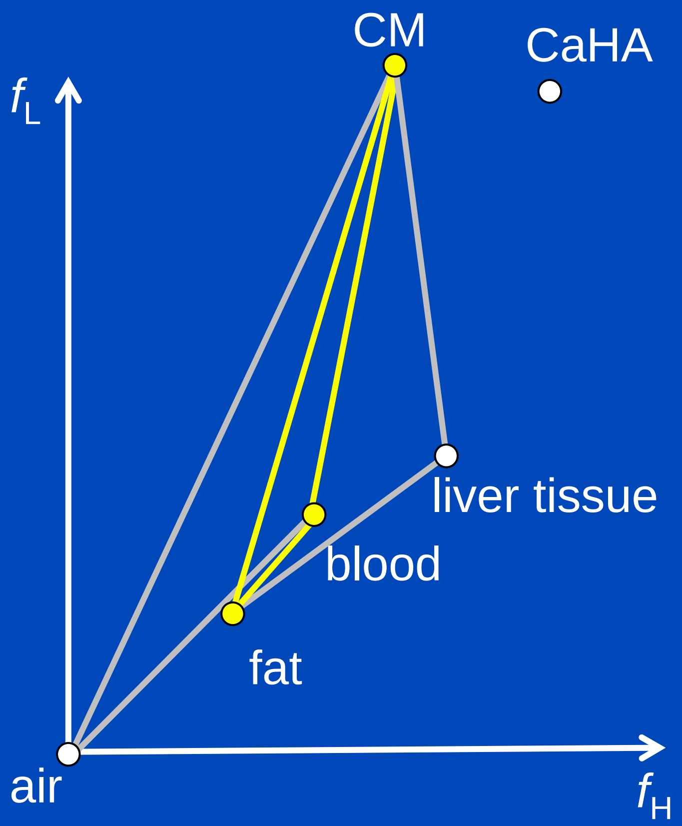

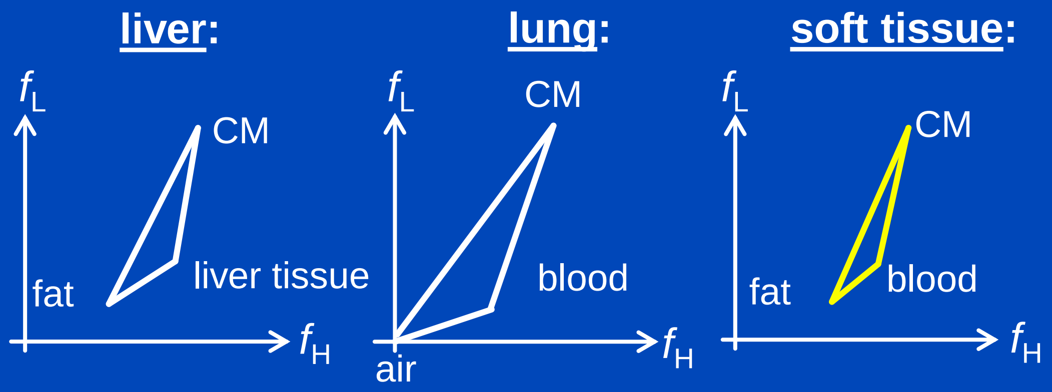

Prior-Based Multi Material Decomposition (PBMMD)

- **Basis materials are adapted to the organ of interest**
- **Overlapping triangles in the DE space**

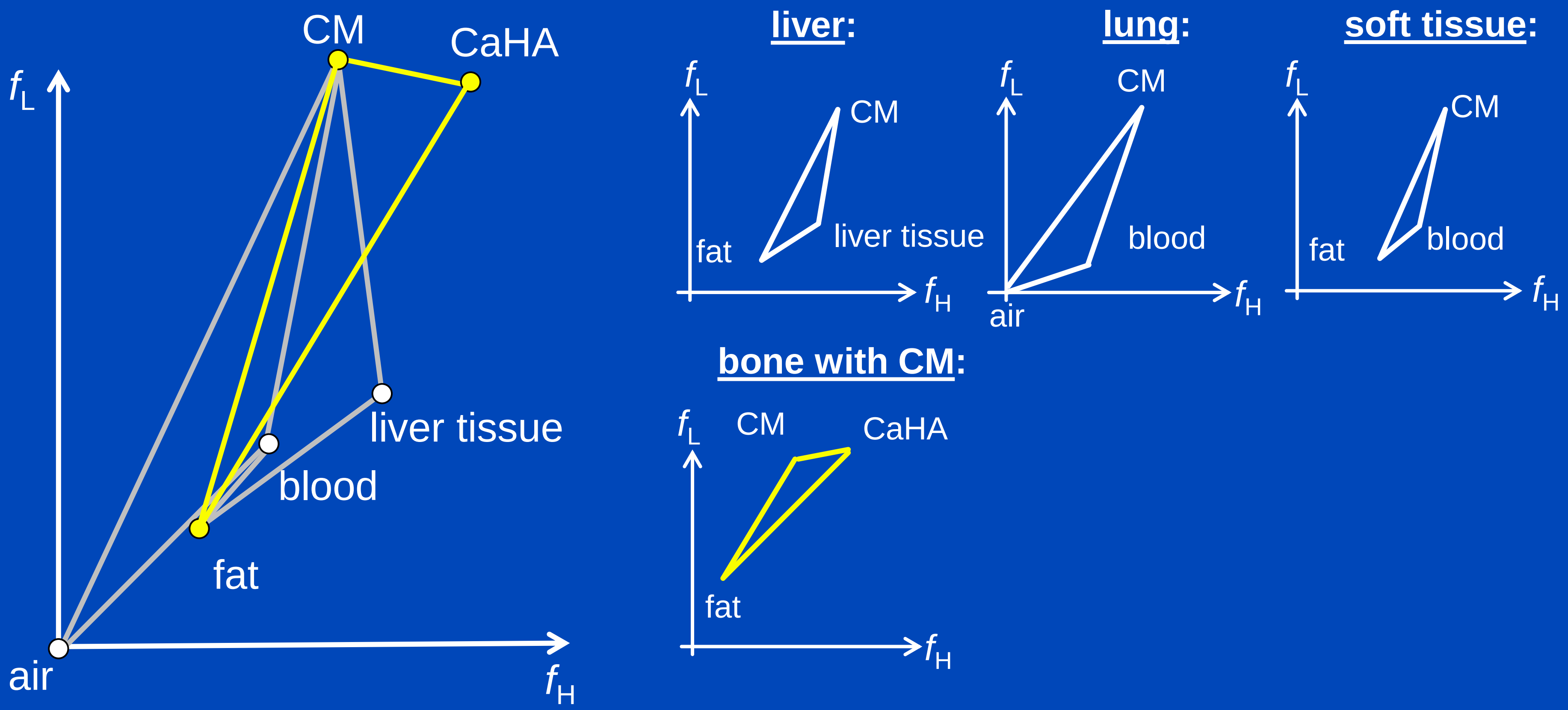

Prior-Based Multi Material Decomposition (PBMMD)

- **Basis materials are adapted to the organ of interest**
- **Overlapping triangles in the DE space**

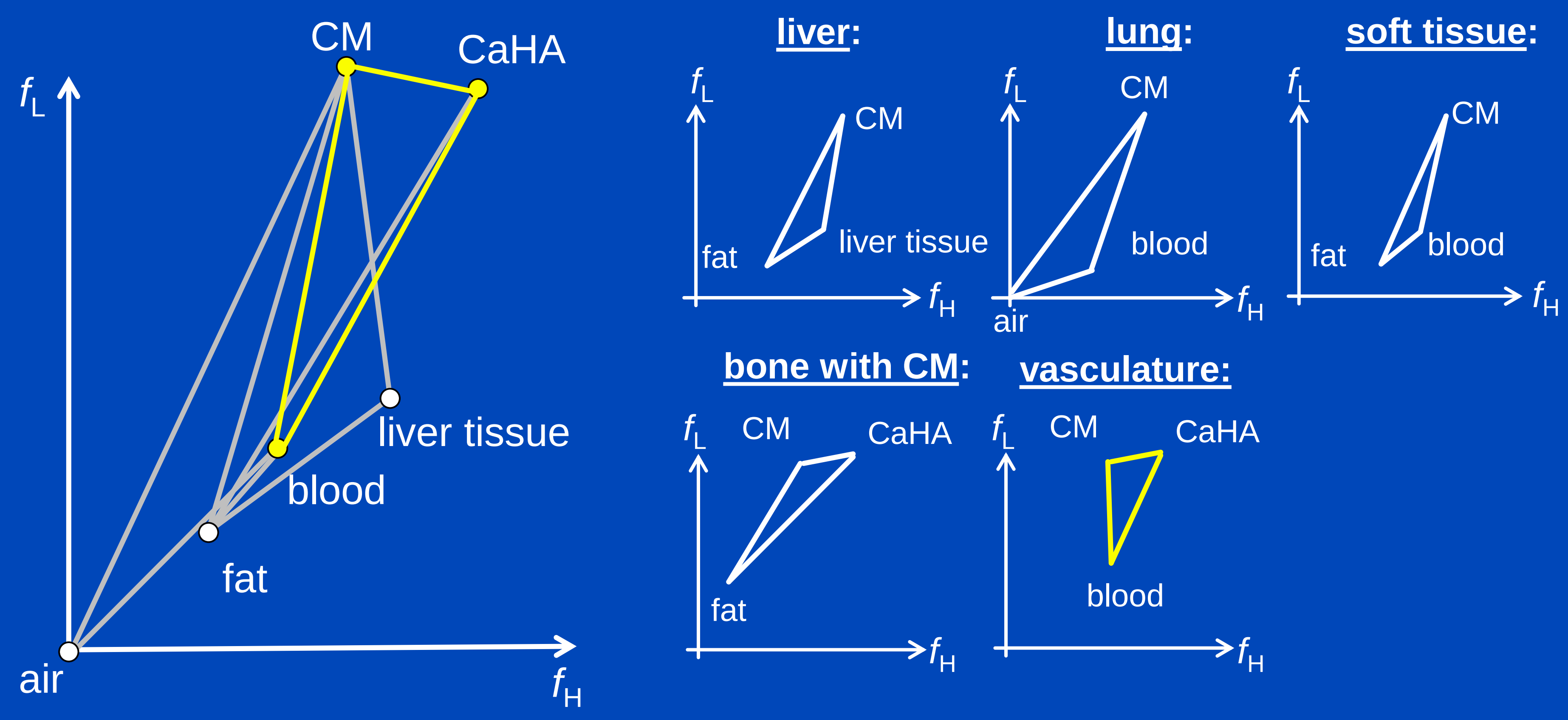

Prior-Based Multi Material Decomposition (PBMMD)

- **Basis materials are adapted to the organ of interest**
- **Overlapping triangles in the DE space**

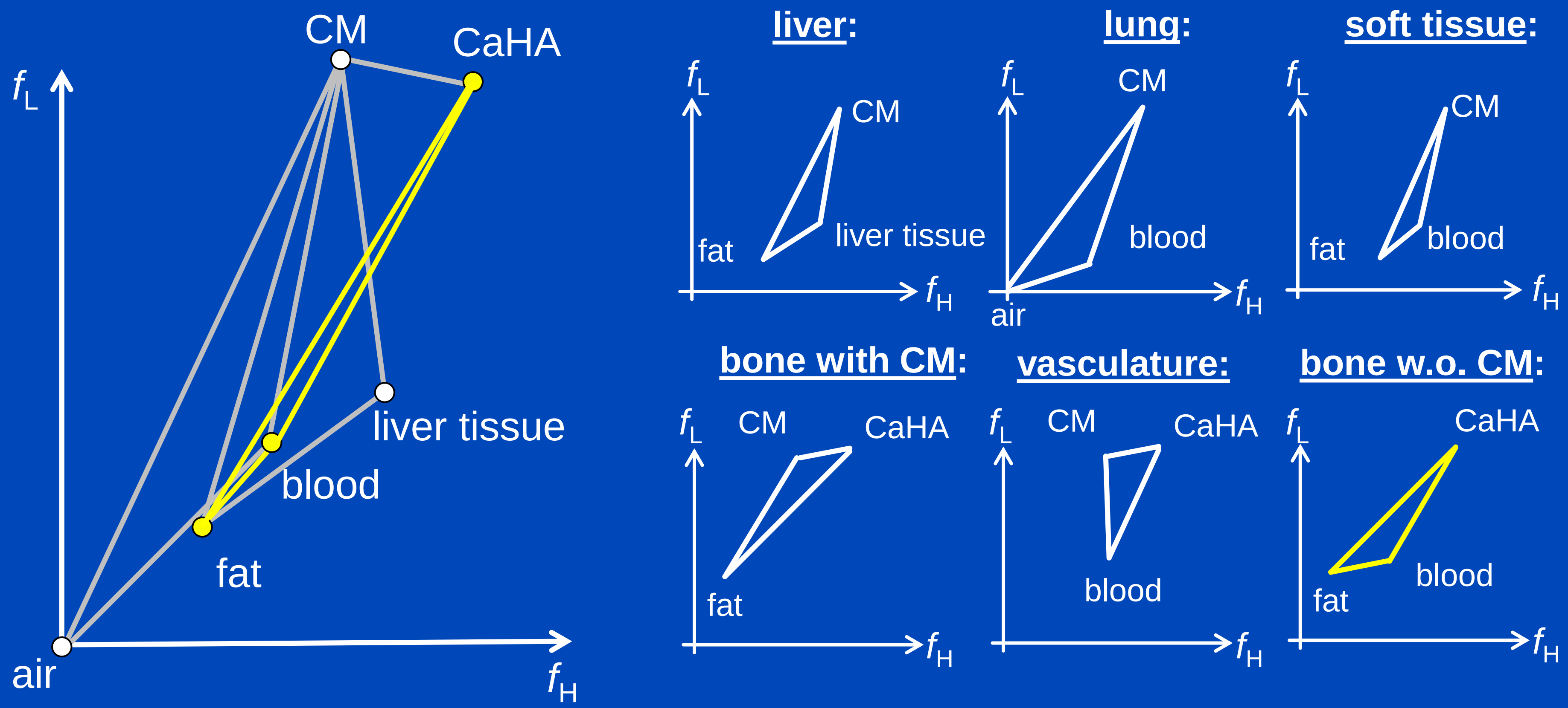

Prior-Based Multi Material Decomposition (PBMMD)

- **Basis materials are adapted to the organ of interest**
- **Overlapping triangles in the DE space**

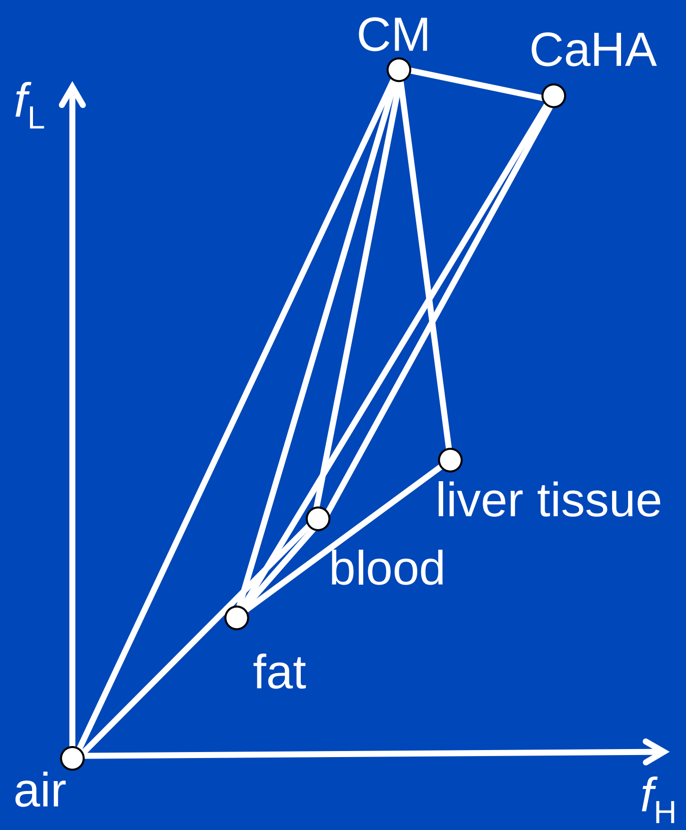

Organ	Basis material library		
	material 1	**material 2**	**material 3**
lung	air	blood	contrast media (CM)
liver	fat	liver tissue	CM
bone	fat	CM	CaHA
muscles	fat	soft tissue	CM
fatty tissue	fat	blood	CM
vasculature	blood	CM	CaHA
spleen, kindeys	fat	blood	CM
…	…	…	…

→We assign one basis material triplet to each voxel

Basis Materials Simulation

– **Fat, soft tissue, liver tissue, blood and air are preset as tabulated in the literature (EPDL)**

ψ	**blood**	**liver**	**soft tissue**	**CM**	**cortical bone**	**air**	**fat**
low energy	59 HU	56 HU	44 HU	14068 HU	854 HU	-1000 HU	-91 HU
high energy	52 HU	51 HU	48 HU	4138 HU	434 HU	-1000 HU	-60 HU

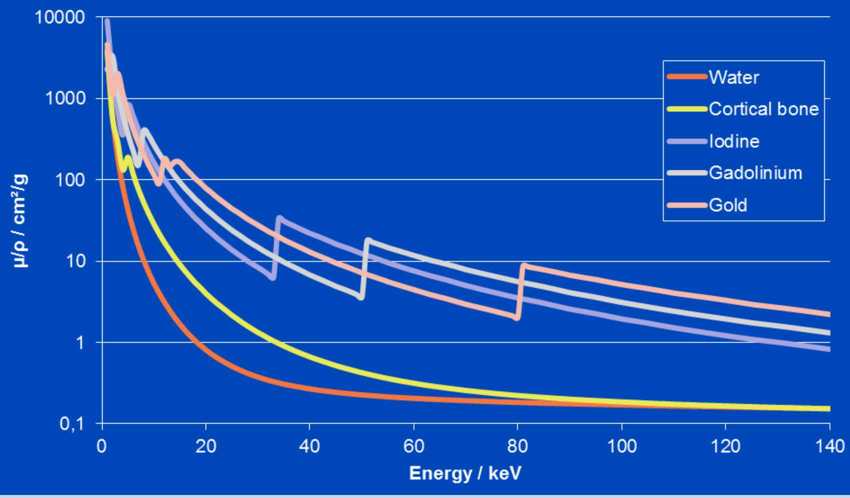

CM Ultravist 370: 370 mg iodine/mL

Cortical bone: 500 mg CaHA/mL

dkfz.

Results
Example Patient I

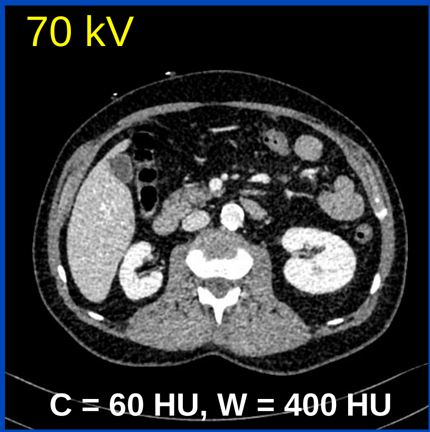

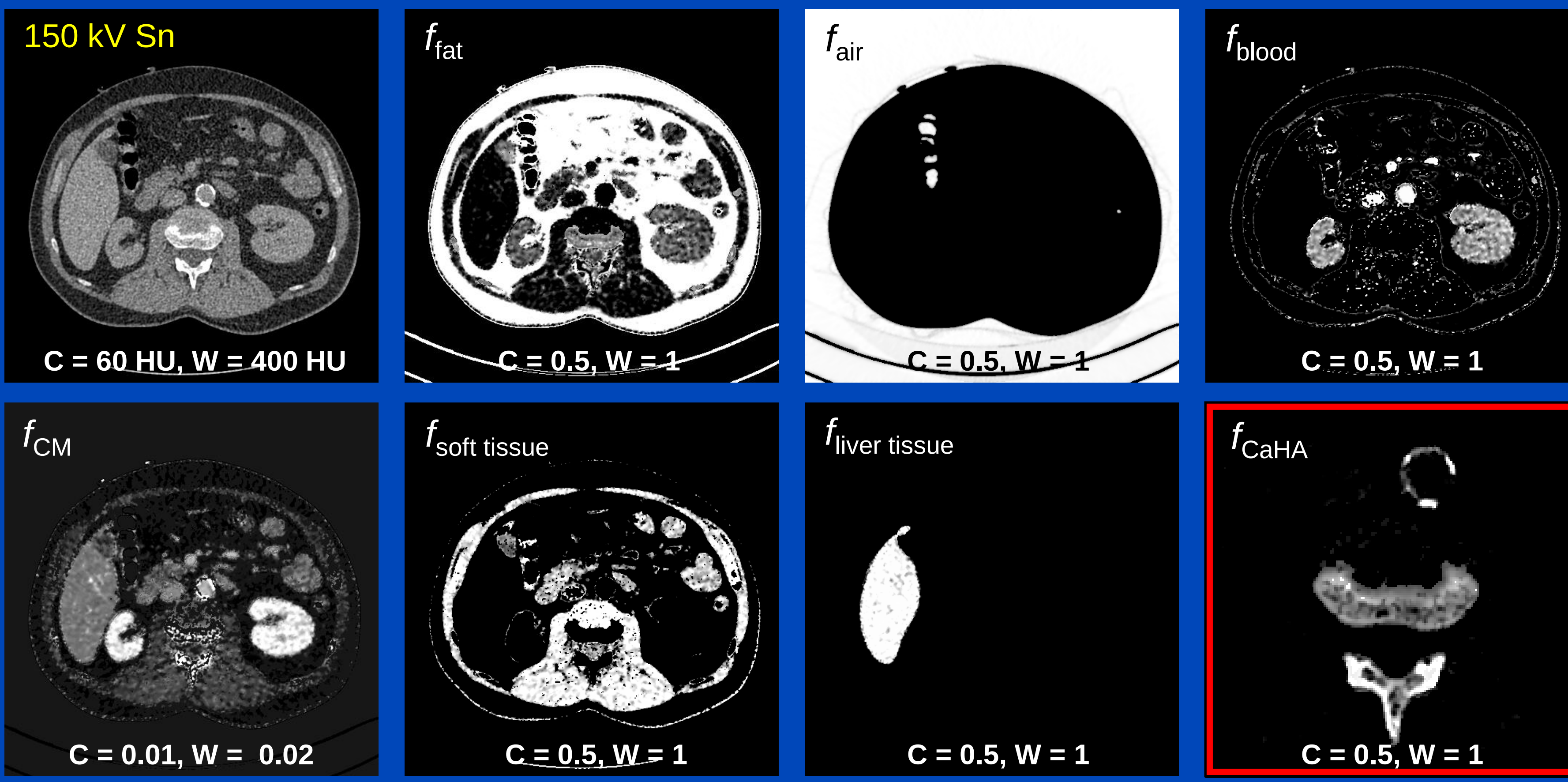

Denoising of the input images (CM: 370 mg/mL, CaHA: 500 mg/mL)

dkfz.

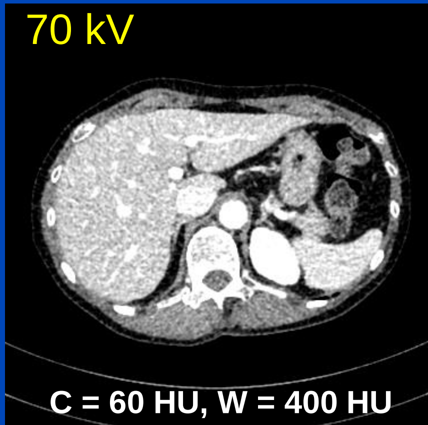

Results
Example Patient II

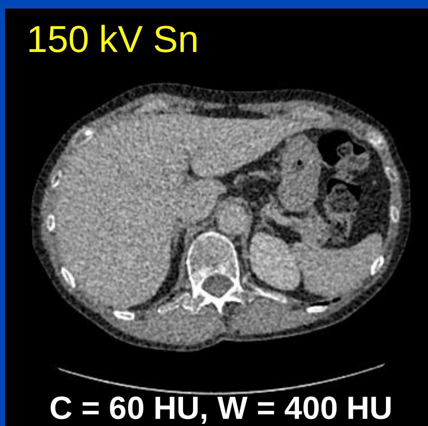

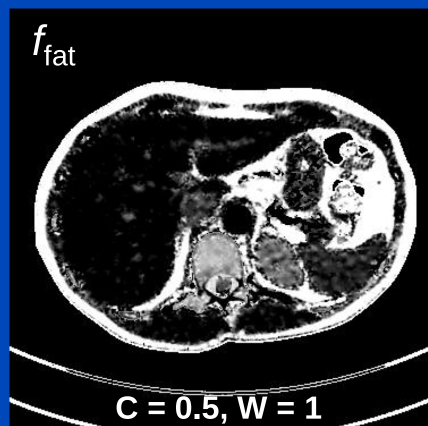

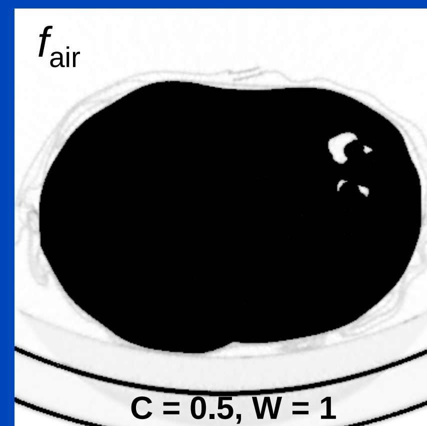

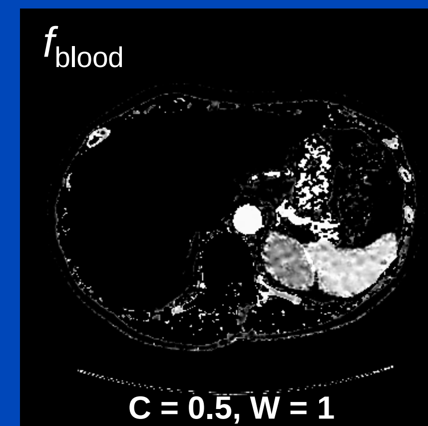

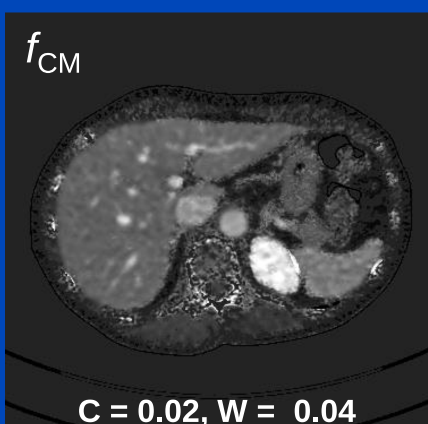

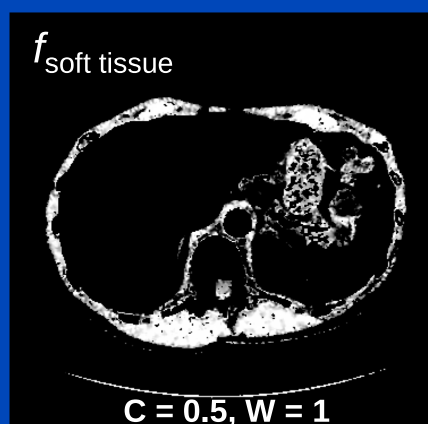

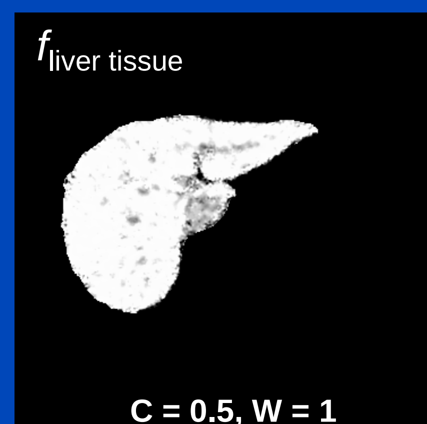

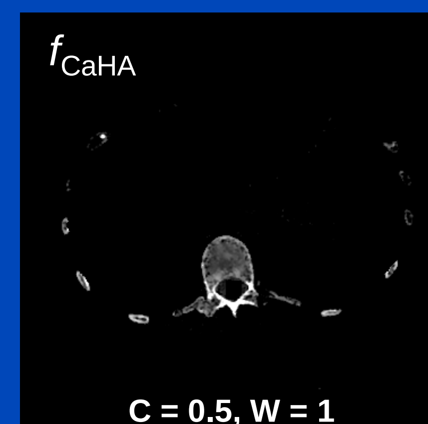

Denoising of the input images (CM: 370 mg/mL, CaHA: 500 mg/mL)

Results

- **Iodine quantification**
- **Location-dependent mass concentration of any material**

$$\gamma(\boldsymbol{r}) = \frac{m}{V} = f_{\text{basis}} \cdot \rho_{\text{basis}}.$$

- **Mass concentration of iodine**

$$\gamma_{\text{iodine}}(\boldsymbol{r}) = f_{\text{CM}} \cdot 370 \text{ mg/mL}$$

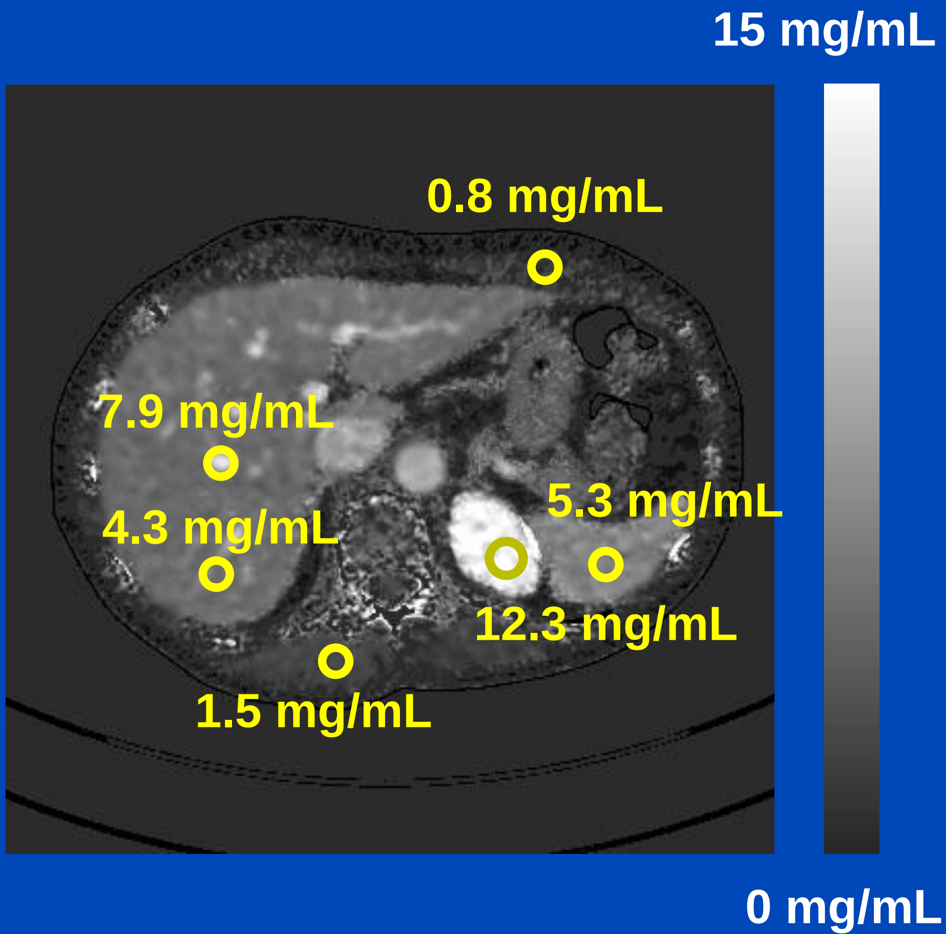

Results

Mixed image

VNC image

Color overlay of iodine map

$$f_{\mathrm{VNC}}(\boldsymbol{r}) = f_{\mathrm{mix}}(\boldsymbol{r}) - w \cdot \gamma_{\mathrm{iodine}}(\boldsymbol{r})$$

$w:$ conversion factor mg/mL in HU

ROI Evaluation and Material Scores

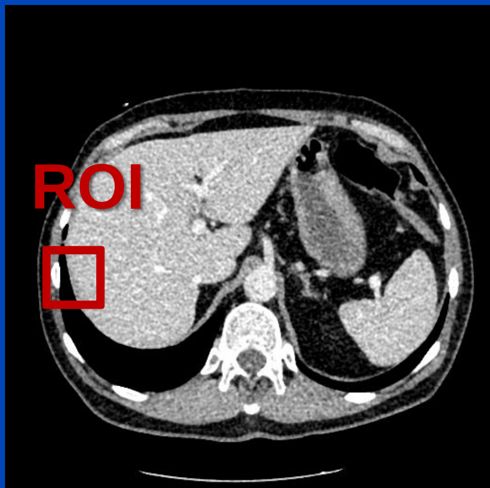

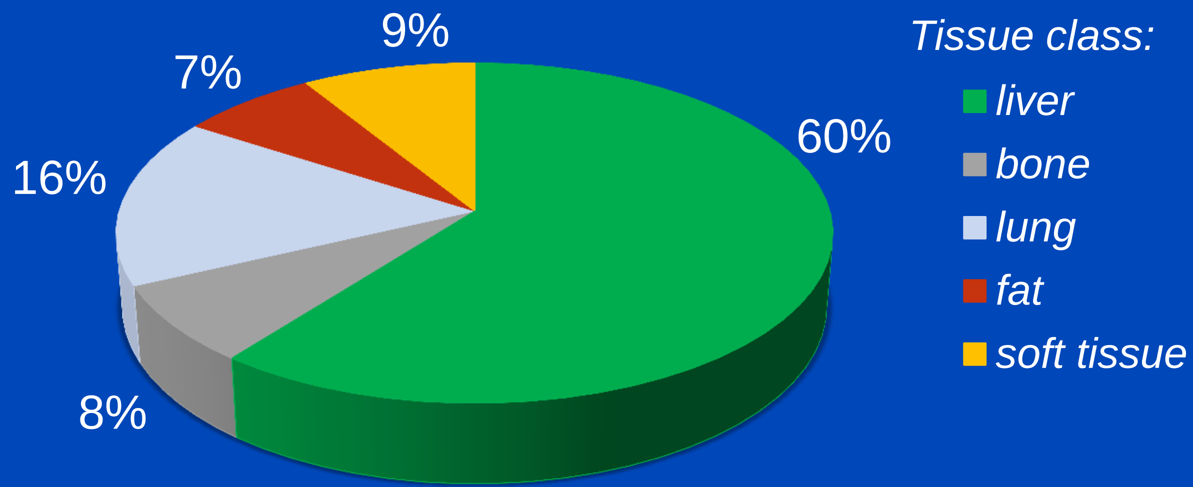

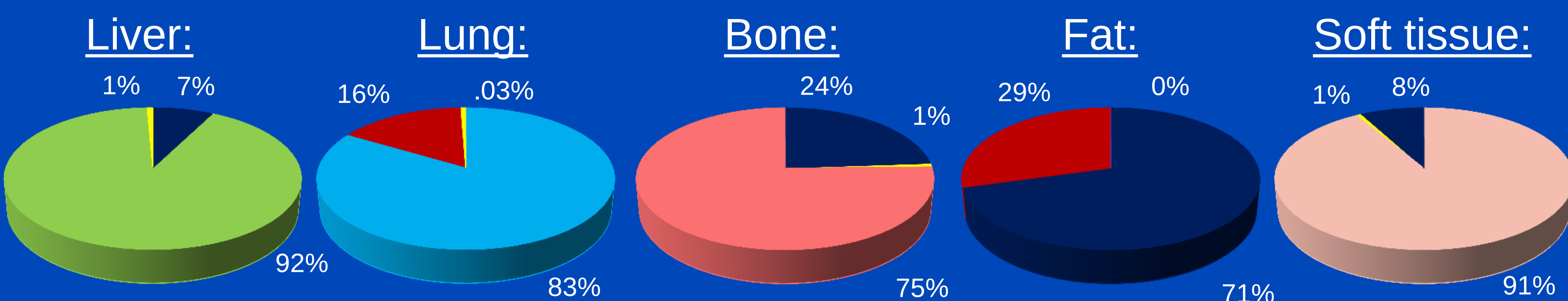

Iodine concentration:

2.59 mg/mL | 0.074 mg/mL | 2.96 mg/mL | 0.00 mg/mL | 1.11 mg/mL

Volume fractions:

CM | *liver tissue* | *fat* | *air* | *CaHA* | *blood* | *soft tissue*

Conclusions

- It can be advantageous to perform DECT material decomposition in an organ-specific manner.
  - Location information enhance the decomposition results
- PBMMD is able to decompose DE data in more than 3 basis materials.
- DE data are decomposed into their material compounds according to the anatomical region they belong to.
- Patient-specific calibration of the basis materials might improve the decomposition accuracy.

Thank You!

This study was supported by the Deutsche Forschungsgemeinschaft (DFG) under grant KA 1678/20-1, LE 2763/2-1 and MA 4898/5-1.

This presentation will soon be available at www.dkfz.de/ct.

Job opportunities through DKFZ's international PhD or Postdoctoral Fellowship programs (www.dkfz.de), or directly through Marc Kachelriess (marc.kachelriess@dkfz.de).

Parts of the reconstruction software were provided by RayConStruct® GmbH, Nürnberg, Germany.